CALCIUM PHOSPHATE FROM WASTE ANIMAL BONES: PHASE IDENTIFICATION ANALYSIS

A.R. Toibah[1], F. Misran[1], Z. Mustafa[1], A. Shaaban[1] and S.R. Shamsuri[2]

[1]Fakulti Kejuruteraan Pembuatan,
Universiti Teknikal Malaysia Melaka, Hang Tuah Jaya, 76100 Durian Tunggal, Melaka, Malaysia.

[2]Department of Material Science and Engineering, Kyoto University, Kyoto 606-8501, Japan.

Corresponding Author's Email: [1]toibah@utem.edu.my

Article History: Received 18 January 2018; Revised 15 June 2018; Accepted 21 September 2018

ABSTRACT: Calcium phosphate bioceramic forms are widely being developed in biomedical applications due to their excellent biocompatibility, bioactivity and osteoconduction characteristics. Apart from synthesized from egg shell wastes, calcium phosphates can be extracted from animal bones. In this study, natural calcium phosphate was extracted by calcination of three different animal bones, which are cow (bovine), goat (caprine) and chicken (galline). The crystallinity and phase identification from FTIR spectrum and XRD patterns were discussed in this paper. Calcium phosphate structures were confirmed through the presence of PO_4^{3-} and OH^- bands as observed by FTIR analysis. FTIR spectra also showed that the organic substances are eliminated in the as-calcined bones at 1000°. XRD results revealed that the as-calcined bones were biphasic calcium phosphate which was verified with relative intensity ratio. The crystallite sizes of the extracted calcium phosphates were estimated to be less than 90nm. Moreover, this study revealed that caprine bones showed the highest HA phase present, followed by bovine and galline bones.

KEYWORDS: *Calcium Phosphate; Hydroxyapatite; Bioceramic; Calcination*

1.0 INTRODUCTION

Bioceramic material have recently been explored particularly in the applications of bone tissue engineering as they have potentials as scaffolds that encourage regeneration of diseased and damaged hard tissues [1]. Calcium phosphates (CP), such as hydroxyapatite (HA)

and tricalcium phosphate (TCP), are accepted bioceramics due to the bioactive and biocompatible properties of HA that allows bonding with the surrounding tissues whereas TCP has a higher rate of biodegradation and subsequently influence the resorbing capacity compared to HA [2]. Consequently, they induce faster bone growth [3]. Hard tissue or bone replacements are synthesized mainly from bioactive materials, which have similar chemical and phase structures with natural bone minerals; biological HA [4].

CP can be extracted from calcium carbonate-based natural materials such as eggshells [5], cockles [6], seashells [7], snail shells [8], oyster shells [9], cuttlefish shells [10] and coral [11]. These raw materials are processed to obtain pure calcium oxide (CaO) and then used as precursors to synthesize calcium phosphates.

Other biogenic materials are calcium phosphate-based wastes which are animal bones [12-14], animal teeth [15] and fish scales [16] where natural calcium phosphates can be directly extracted through calcination procedures or termed as thermal decomposition method. The subject of study and the extraction method chosen were economical and support global sustainability. Other methods of extraction methods recorded are subcritical water process and alkaline hydrothermal hydrolysis [12].

Bones and teeth of animals are composite materials that consist of 65% of inorganic nano-crystalline solid of a basic apatite structure, known as the carbonate-hydroxy-apatite [17]. The other 35% remaining mass are attributed as the organic substances and water. Natural CPs, such as bones and teeth, are considered as the impure forms of HA. Possible replacements are potassium, magnesium, strontium and sodium in place of calcium ions, carbonate instead of phosphate ions and chloride or fluoride at the hydroxyl ions [18].

Biological apatites are usually more nonstoichiometric and less crystalline at the early stage to inspire important elements necessary for growth and they gradually form to become the stoichiometric Ca/P ratio of 1.67 and more crystalline that restricts interchange [17]. This paper recapitulates the CP extracted from several animal bones, which are bovine (cow), caprine (goat) and galline (chicken) bones.

The present study focuses on the structural characterizations on the as-calcined bone by X-Ray Diffraction (XRD) and Fourier Transform Infrared Spectroscopy (FTIR).

2.0 METHODOLOGY

2.1 Animal Bones Preparation

The waste animal bones from bovine (BB), caprine (CB) and galline (GB) were collected from local restaurants and washed thoroughly with water and distilled water to remove the organic substances. The cleaned bone samples were repeatedly boiled in distilled water to detach the flesh from the bones. Then, the raw bones were dried at 120°C for 24 hours and crushed using pestle and mortar.

2.2 Thermal Decomposition

The crushed powder was thermally treated in furnace (Front Loading Chamber Furnace, Carbolite UK) at air atmosphere and temperature of 1000°C for 3 hours of holding time and 5°C/min of heating and cooling rate to eliminate all organic constitutes of the inner parts of the bones.

2.3 Characterization

Fourier transform infrared (FTIR) spectroscopy (Jasco, FT/IR 6100) was performed in order to understand the phase changes upon calcination and to determine HA stoichiometry deviations, i.e. the presence of anions and substituting PO_4^{3-} and OH^- groups. The identification of the crystalline phase of the as-calcined powders were measured using X-ray Diffraction (XRD, PANalytical, System X'Pert Pro) by comparing the experimental XRD patterns to the provided Joint Committee on Powder Diffraction Standards (JCPDS) card number 09-0432 for HA and 055-0898 for β-TCP. The peaks of XRD diffraction pattern was used to estimate the crystallite size (D) using the Scherer's formula as shown in Equation (1) [19]:

$$D = \frac{K\lambda}{B\cos\theta} \quad (1)$$

where D obtained will be in nanometer, λ is the wavelength of the incident radiation, K is the Scherer's constant which equals to 0.94, θ is the diffraction angle and B is the full width at half maximum (FWHM) of X-ray reflection in radians.

The degree of crystallinity, X_c can be evaluated by the following relation using Equation (2):

$$X_c = 1 - \frac{V_{112/300}}{I_{300}} \quad (2)$$

$V_{112/300}$, which represents the intensity of the valley between peaks (112) and (300), is divided with intensity of peak (300) [20]. Finally, the phase identification was determined from the relative intensity ratio (RIR) of HA to β-TCP using the intensities of the peaks respective phase and calculated by Equation (3) [2]:

$$RIR = \frac{I\beta\text{-}TCP}{I_{\beta\text{-}TCP} - I_{HA}} \quad (3)$$

3.0 RESULTS AND DISCUSSION

The elimination of the organic material of the bones was observed with the distinctive color change. The crushed raw bones were brown in color while after calcined at 1000°C, the color changed to white as indication of HA, suggesting complete removal of organic substances [15]. Similar white colored samples were obtained by heating tuna bones at the range of 800 - 1200°C showing removal of the organic matrix leaving the inorganic bone mineral [13].

The FTIR spectrum of all animal bones which consists of raw animal bone and CP extracted from calcined bones at 1000°C are shown in Figure 1. Animal bones are composed of the organic and inorganic part. The organic part can be identified mainly as collagen fibers which are proteins [12]. FTIR was able to examine the elimination of organic substance and water from raw bones by the examination of certain bonds available in as-produced HA.

Protein can be noticed by FTIR through the investigation of amide regions as shown in the spectrum (Figure 1 (a)-(c)). There were additional bands found at the spectra of raw bones specifically in the shaded area showing two (amide I and II) of three main regions of amide found between bands ~1520 to ~1690cm^{-1}. Previous studies reported that amide III bands were seen at the second derivative of FTIR spectra in the range of ~1200 to ~1290cm^{-1} [12]. However, the

results obtained in this study shows that the amide III bands do not appear in the spectra of the as-calcined bones due to the high calcination temperature that used in this study. Hence, all animal bones produced pure CP structures after calcined at 1000°C.

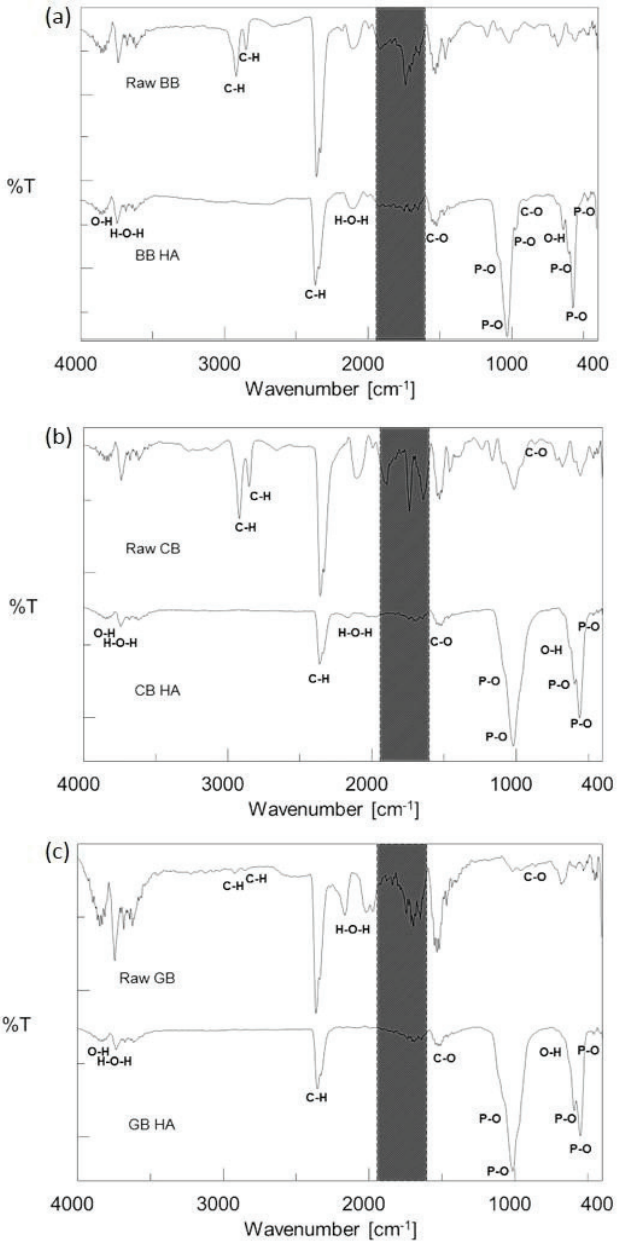

Figure 1: FTIR Spectra for raw bones (Raw) and as-calcined bone (HA) samples at 1000°C from different types of animal bones

The lower intensity of hydroxyl (OH^-) stretching at ~3570 cm^{-1} and also the absence of C-H bands or organic material at ~2920 and ~2850 cm^{-1} [20] of the as-calcined animal bones compared to the raw bones demonstrate the elimination of water and organic substances after the bones were calcined at 1000°C. Water bands of chicken bones (GB, Figure 1 (c)) showed distinctive reduction after the heat treatment. However, CB sample shows the most intense peak of C-H bands, while GB displays the lowest.

The main indication of HA can be identified by the characteristic bands of PO_4^{3-} group at three regions (Figure 2). All phosphate stretching vibration modes were represented at the range of ~960 to ~1100 cm^{-1} as the first region, between ~570 to ~630 cm^{-1} as the second region and lastly at ~470 cm^{-1} was the third region. In the first region, the phosphate band specifically found at ~1080 cm^{-1} represented the presence of TCP [2]. Previous studies obtained no obvious peak from FTIR analysis for pure HA within this area [12]. The declination of carbonate (C-O) peak, located at ~1500cm^{-1}, shows pure CP with both phases of bone extraction. No bands characterized as acid phosphate (HPO_4^{2-}) was found at the range of ~530 to ~540 cm^{-1} in the FTIR spectra verifying the extraction of a matured bone mineral [5].

FTIR analysis can also identify the condition of carbonate ions incorporated into the HA structure. There are two classifications, A-type and B-type carbonated HA. A-type incorporation is when CO_3^{2-} substitutes OH^- and reported to have low affinity reactions towards human cells and low collagen production [20]. Carbonate ions at band ~1540 cm^{-1} shows A-type carbonated HA [21], while bands ~1420 and ~1460 cm^{-1} of carbonate were associated to the partial PO_4^{3-} replacement (B-type). B-type substitution was clearly shown by FTIR spectra for HA extracted from bovine bones (Figure 1 and 2). Therefore, HA extracted from animal bones are AB-type carbonated HA which was similar to the results obtained by other studies on fish bones [20].

Figure 3 shows the selected phases available in the HA sample powders for the respective animal bones verifying their chemical structures. The main peaks were screened with high intensity peaks from the JCPDS 09-0432 (HA) and 055-0898 (β-TCP) peak lists. As seen in Figure 3 for all samples, the XRD spectra of the as-calcined bones have distinctive peaks compared to the raw bones which may confirm the elimination of organic substance [12] and high degree of crystallinity [20].

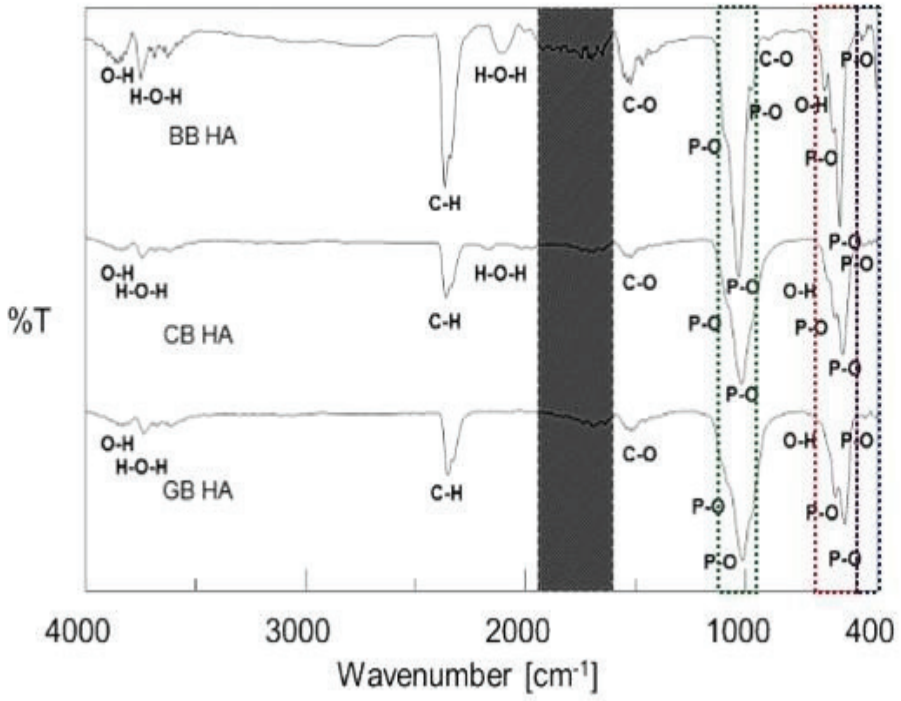

Figure 2: FTIR spectra for all HA extracted from animal bones calcined at 1000°C

Calcination of the raw bones have stabilized the crystallization and grain growth of the HA structure which is indicated by the sharp and narrow XRD peaks [22]. Results obtained in this study also revealed that the samples calcined at temperature of 1000 °C possess higher crystallinity than the raw animal bones as shown in Figure 3. Figuiredo et.al also reported in their study that crystallinity of bone samples increases as the calcination temperature increases [23].

For further calculations of XRD analysis, data from raw animal bones were excluded because of the indefinite peaks recorded caused by the dispersion of X-ray radians by the organic matrix and collagen fibers present [12]. The 2θ position and intensity of the main peaks of the as-calcined bone samples were summarized in Table 1. Most β-TCP peaks and with consistently highest intensity was found in HA from calcined GB HA samples followed by BB HA and finally CB HA as shown in Figure 3.

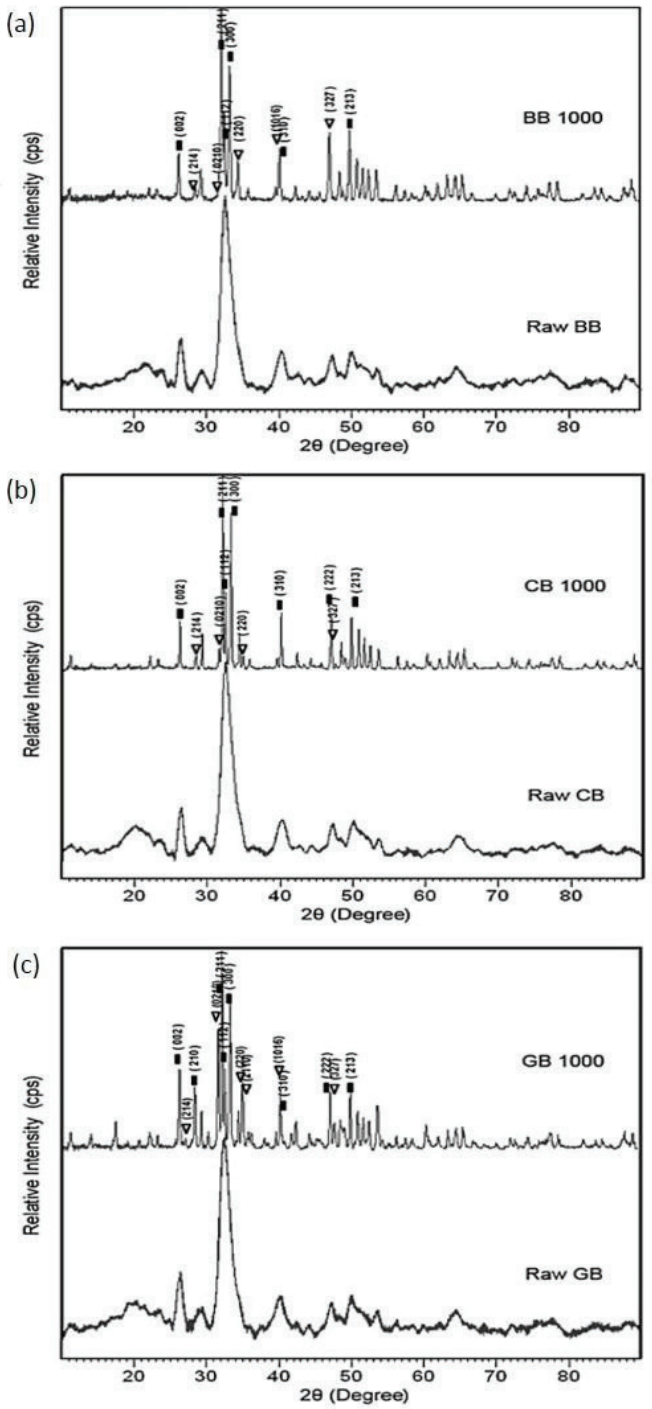

Figure 3: XRD pattern of raw bones and as-calcined bones at 1000°C from different types of animal bones [▽ β-TCP; ∎ HA]

Table 1: X-ray diffraction spectra of HA obtained from thermally treated animal bones

Planes (h k l)	Angle, 2θ (°)	Intensity (%)	BB		CB		GB	
			2θ (°)	I (%)	2θ (°)	I (%)	2θ (°)	I (%)
HA 09-0432								
0 0 2	25.879	40	26.106	28.880	26.226	27.130	26.263	41.850
2 1 1	31.774	100	32.005	100.000	32.117	100.000	32.145	100.000
1 1 2	32.197	60	32.483	44.990	32.539	40.880	32.573	41.870
3 0 0	32.902	60	33.129	67.460	33.248	80.630	33.268	75.190
3 1 0	39.819	20	40.121	26.680	40.133	29.030	40.291	16.550
2 2 2	46.713	30	n. a.	n. a.	47.019	28.500	47.049	28.640
2 1 3	49.469	40	49.739	35.900	49.809	26.710	49.836	28.410
Total Error			0.045	1.089	0.067	1.818	0.076	1.109
TCP 055-0898								
2 1 4	27.805	53	28.161	9.430	28.296	8.380	28.341	32.650
0 2 10	31.027	100	n. a.	n. a.	31.631	12.100	31.585	60.430
2 2 0	34.371	65	34.333	23.000	34.949	8.210	34.921	33.460
3 2 7	46.984	30	46.905	33.120	47.161	13.140	47.188	14.560
Total Error			0.024	1.572	0.058	3.157	0.077	1.780

Apart from dehydroxylation of HA [21], the presence of β-TCP as the secondary phase acts as impurity to the main phase; HA [24]. This was shown in Figure 3 and Table 1 where slight shifting of the peaks were observed. The relative errors were evaluated with respect to the true value and totaled up according to Equation (4) [22]:

$$\text{Total Error} = \frac{\left|\text{True value} - \text{Measured value}\right|}{\text{True value}} \tag{4}$$

From the total errors calculated, HA extracted from BB (2θ position = 0.045, 0.045 and intensities = 1.089, 1.572) has the most similar peaks with HA standard.

Table 2 displays the calculated crystallite size and degree of crystallinity of all extracted HA samples. Line broadening of peak (211) was chosen to evaluate the crystallite size because this peak was well distinguished. The crystallite sizes of HA from animal bones are less than 90 nm in the ascending order of GB < CB < BB. Other reports on HA extracted from animal bones also obtained similar crystallite sizes [23].

Table 2: Crystallite Size (D) and Degree of Crystallinity (X_c)

Sample	D (nm)	Xc (%)
BB HA	84.63	0.667
CB HA	57.33	0.507
GB HA	38.48	0.557

In general, HA from animal bone naturally has less crystallinity compared to HA obtains from synthesis route [17, 20]. This is due to the processing parameters such as higher temperature and pressure that used during the synthesis method. The estimated degree of crystallinity of each sample did not show much difference between each other, but in an altered ascending sequence of CB < GB < BB probably, this sequence was influenced by other factors such as the presences of other phases within the HA matrix. With the particular potentials of biphasic calcium phosphate (mixture of HA and β-TCP) currently as synthetic biomaterials, the relative intensity ration (RIR) of these heat-treated animal bones was determined. Due to the absent (0210) peak of β-TCP from BB sample, another set of close peaks were selected, (300) at 2θ, 32.902° (HA JCPDS 09-0432) for HA and (220) at 2θ, 34.371° (β-TCP JCPDS 055-0898) for β-TCP from Table 1 was used to calculate the RIR of HA to β- TCP. Table 3 summarized the RIR values.

Table 3: RIR values of HA to TCP in the animal bone powders

Sample	HA: TCP
BB HA	74.57: 25.43
CB HA	90.76: 9.24
GB HA	69.2: 30.8

These results synchronize with the intensities summarized in Table 1 and the XRD patterns as represented in Figure 3. After the calcination at 1000°C, it can be concluded that GB has produced the highest amount of TCP phase compared to other animal bones. Hence, the HA extracted from these animal bones formed biphasic calcium phosphate structures instead of HA phase alone.

4.0 CONCLUSION

Extraction methods of biological apatite from animal bone bio-wastes by thermal decomposition researches as this study support global sustainability. The use of bio-waste is economical and helps to manage human daily consumption and disposal of food from animal meat as cow, goat and chicken. The analysis accomplished confirms the biphasic calcium phosphate structure consisting of HA and β-TCP phases from as-calcined animal bones. FTIR spectra verify the AB-type carbonated HA extracted from all animal bones. XRD analysis confirms the crystallite sizes of <90 nm for calcium phosphates were achieved by calcination at 1000°C. The natural biphasic structure obtained can be utilized to develop biomaterial implants that can be one of the components to perform bone tissue engineering initiatives. Accompanying researches should be focus on the mechanical properties and biological responses of these extracted natural HA to facilitate further clinical researches.

ACKNOWLEDGMENTS

The authors appreciatively acknowledged the technical assistance from the staffs in Faculty of Manufacturing Engineering, University Technical Malaysia Melaka and financial supports provided, Project No. PJP/2010/FKP (25A) S00758 and PJP/2011/FKP (12B) S00879.

REFERENCES

[1] F. Baino, S. Caddeo, G. Novajra and C. Vitale-Brovarone, "Using porous bioceramic scaffolds to model healthy and osteoporotic bone", *Journal of the European Ceramic Society*, vol. 36, no. 9, pp. 2175-2182, 2016.

[2] M. Ebrahimi, M.G. Botelho and A. V. Dorozhkin, "Biphasic calcium phosphates bioceramics (HA/TCP): Concept, physicochemical properties and the impact of standardization of study protocols in biomaterials research", *Materials Science and Engineering: C,* vol. 71, pp. 1293–1312, 2017.

[3] R. Z. LeGeros, A. Ito, K. Ishikawa, T. Sakae and J. P. LeGeros, *Advanced Biomaterials Fundamentals, Processing and Applications*. New Jersey: John Wiley & Sons, 2009.

[4] G. Turnbull, J. Clarke, F. Picard, P. Riches, L. Jia, F. Han, B. Li, and W. Shu, "3D bioactive composite scaffolds for bone tissue engineering", *Bioactive Materials*, vol. 3, no. 3, pp. 278-314, 2018.

[5] G. Gergely, F. Weber, I. Lukacs, A. L. Toth, Z. E. Horvath, J. Mihaly and C. Balazsi, "Preparation and characterization of hydroxyapatite from eggshell", *Ceramic International*, vol. 36, no. 2, pp. 803-806, 2010.

[6] M. Akram, R. Ahmed, I. Shakir, W. A. W. Ibrahim and R. Hussain, "Extracting hydroxyapatite and its precursor from natural resources", *Journal of Materials Science*, vol. 49, no. 4, pp. 1461-1475, 2014.

[7] X. Zhang and K. S. Vecchio, "Creation of dense hydroxyapatite (synthetic bone) by hydrothermal conversion of seashells", *Materials Science and Engineering C*, vol. 26, no. 8, pp. 1445-1450, 2006.

[8] A. Singh and K. M. Purohit, "Chemical synthesis, characterization and bioactivity evaluation of hydroxyapatite prepared from garden snail (Helix Aspersa)", *Journal of Biotechnology and Biomaterials*, vol. 1, no. 2, pp. 1-5, 2011.

[9] S. C. Wua, H. C. Hsua, Y. N. Wuc and W. F. Hoc, "Hydroxyapatite synthesized from oyster shell powders by ball milling and heat treatment", *Materials Characterization*, vol. 6, no. 2, pp. 1180-1187, 2011.

[10] J. H. G. Rocha, A. F. Lemos, S. Agathopoulos, P. Valério, S. Kannan, F. N. Oktar and J. M. F. Ferreira, "Scaffolds for bone restoration from cuttlefish", *Bone*, vol. 37, no. 6, pp. 850-857, 2005.

[11] U. Ripamonti, J. Crooks, L. Khoali and L. Roden, "The induction of bone formation by coral-derived calcium carbonate / hydroxyapatite constructs", *Biomaterials*, vol. 30, no. 7, pp. 1428–1439, 2009.

[12] N. A. M. Barakat, M. S. Khil, A. M. Omran, F. A. Sheikh and H. Y. Kim, "Extraction of pure natural hydroxyapatite from the bovine bones bio waste by three different methods", *Journal of Materials Processing Technology*, vol. 209, no. 7, pp. 3408-3415, 2009.

[13] J. Venkatesan and S. K. Kim, "Effect of temperature on isolation and characterization of hydroxyapatite from tuna (Thunnus Obesus) bone", *Materials*, vol. 3, no. 10, pp. 4761-4772, 2010.

[14] C. Y. Ooi, M. Hamdi, S. Ramesh, "Properties of hydroxyapatite produced by annealing of bovine bone", *Ceramics International*, vol. 33, no. 7, pp. 1171-1177, 2007.

[15] A. Elkayar, Y. Elshazly and M. Assaad, "Properties of hydroxyapatite from bovine teeth", *Bone Tissue Regeneration Insights*, vol. 2, no. 7, pp. 31-36, 2009.

[16] Y. C. Huang, P. C. Hsiao and H. J. Chai, "Hydroxyapatite extracted from fish scales, effect on MG63 osteoblast-like cells", *Ceramics International*, vol. 37, no. 6, pp. 1825-1831, 2011.

[17] M. Vallet-Regí and D. Arcos, *Biomimetic Nanoceramics in Clinical Use from Materials to Application*. Cambridge: RSC Publishing, 2008.

[18] D. L. Bartel, D. T. Davy and T. M. Keaveny, *Orthopaedic Biomechanics, Mechanics and Design in Musculoskeletal Systems*. New Jersey: Pearson Education, 2006.

[19] Gunawan, I. Sopyan, Suryantoa and A. Naqshbandi, "Zinc-doped biphasic calcium phosphate nanopowders synthesized via sol-gel method", *Indian Journal of Chemistry*, vol. 53A, no. 2, pp. 152-158, 2014.

[20] M. Sadat-Shojai, M. Atai and A. Nodehi, "Design of experiments (DOE) for the optimization of hydrothermal synthesis of hydroxyapatite nanoparticles", *Journal of the Brazilian Chemical Society*, vol. 22, no. 3, pp. 571-582, 2011.

[21] I. S. Neira, Y. V. Kolen'ko, O. I, Lebedev, G. V. Tendeloo, H. S. Gupta, F. Guitian and M. Yoshimura, "An effective morphology control of hydroxyapatite crystals via hydrothermal synthesis", *Crystal Growth and Design*, vol. 9, no. 1, pp. 466-474.

[22] J. Venkatesan, Z. J. Qian, B. M. Ryu, N. V. Thomas and S. K. Kim, "A comparative study of thermal calcination and an alkaline hydrolysis method in the isolation of hydroxyapatite from Thunnus obesus bone", *Biomedical Materials*, vol. 6, no. 3, pp. 35003-35015, 2011.

[23] M. Figueiredo, A. Fernando, G. Martins, J. Freitas, F. Judas and H. Figueiredo, "Effect of the calcination temperature on the composition and microstructure of hydroxyapatite derived from human and animal bone", *Ceramics International*, vol. 36, no. 8, pp. 2383–2393, 2010.

[24] D. C. William, *Materials Science and Engineering an Introduction*. New York: John Wiley & Sons, Inc., 2003.